Earth and Planetary Science Letters 429 (2015) 122–127

Contents lists available at ScienceDirect

Earth and Planetary Science Letters

www.elsevier.com/locate/epsl

Landslide seismic magnitude

C.H. Lin [a,e,f,*], J.C. Jan [b], H.C. Pu [c], Y. Tu [d], C.C. Chen [b], Y.M. Wu [e,f]

[a] Institute of Earth Sciences, Academia Sinica, Taipei, Taiwan
[b] Dept. of Earth Sciences, National Central University, Jhongli, Taiwan
[c] Central Weather Bureau, Taipei, Taiwan
[d] Dept. of Natural History Sciences, Hokkaido University, Japan
[e] Dept. of Geosciences, National Taiwan University, Taipei, Taiwan
[f] National Center for Research on Earthquake Engineering, National Applied Research Laboratories, Taipei, Taiwan

ARTICLE INFO

Article history:
Received 12 January 2015
Received in revised form 28 July 2015
Accepted 30 July 2015
Available online 14 August 2015
Editor: P. Shearer

Keywords:
landslide
seismic magnitude
Hsiaolin landslide
seismic *b*-value
landslide prevention

ABSTRACT

Landslides have become one of the most deadly natural disasters on earth, not only due to a significant increase in extreme climate change caused by global warming, but also rapid economic development in topographic relief areas. How to detect landslides using a real-time system has become an important question for reducing possible landslide impacts on human society. However, traditional detection of landslides, either through direct surveys in the field or remote sensing images obtained via aircraft or satellites, is highly time consuming. Here we analyze very long period seismic signals (20–50 s) generated by large landslides such as Typhoon Morakot, which passed though Taiwan in August 2009. In addition to successfully locating 109 large landslides, we define landslide seismic magnitude based on an empirical formula: $\mathbf{Lm} = \log(A) + 0.55\log(\Delta) + 2.44$, where A is the maximum displacement (μm) recorded at one seismic station and Δ is its distance (km) from the landslide. We conclude that both the location and seismic magnitude of large landslides can be rapidly estimated from broadband seismic networks for both academic and applied purposes, similar to earthquake monitoring. We suggest a real-time algorithm be set up for routine monitoring of landslides in places where they pose a frequent threat.

1. Introduction

Catastrophic landslides can not only destroy many human lives, but also have strong economic, social, and political impacts on many countries. For example, a huge number of landslides were triggered by the extremely heavy rainfall (>3000 mm) caused by the synergistic effect of both Typhoon Morakot and the southwestern monsoon in Taiwan in August 2009 (Lin et al., 2010; Tsou et al., 2011; Kuo et al., 2011). One of the most deadly of these landslides buried 474 residents in the Hsiaolin village of southern Taiwan. Based on a detailed investigation (Chen et al., 2011), the disaster process could be clearly divided into two major parts. First, the landslide buried the northern part of the village at around 10:16PM, August 7, 2009 (UTC time) (Lin et al., 2010) and immediately blocked the Cishan River to form a dam. Only a small group of residents (∼40) who lived at the southern part of the village successfully escaped to high land. All others were not so lucky and an hour later, the collapse of the dam completely swept away the remaining parts of the village without any warning (Tsou et al., 2011; Chen et al., 2011). News of the deadly disaster was not conveyed until more than 24 h later, and the premiere of Taiwan resigned several days later because of the delay in the evacuation and rescue work.

At that time, in fact, there was no reliable way to rapidly detect landslide location or seismic magnitude in order to issue a warning of possible dam failure. Traditionally, landslide detection depends on either detailed on-site reports or aircraft and satellite images from space; however, those methods might not help when telephones and other wireless communication systems are not functioning normally and it is impossible to report any survey results from the field. Also, most aircraft and satellite images are obscured when the weather conditions are extreme, for example during typhoon or monsoon periods. In addition to the rapid detection of landslide location, reliable quantitative estimation of landslide seismic magnitude is important for evaluating the possibly complex impact of disasters. Thus, new methods for rapidly detecting large landslide locations as well as their seismic magnitude should be developed to mitigate associated disasters, such as dam damage and downstream floods.

* Corresponding author at: Institute of Earth Sciences, Academia Sinica, PO Box 1-55, Nankang, Taipei, Taiwan. Tel.: +886 2 27839910x521; fax: +886 2 27839195.
E-mail address: lin@earth.sinica.edu.tw (C.H. Lin).

http://dx.doi.org/10.1016/j.epsl.2015.07.068

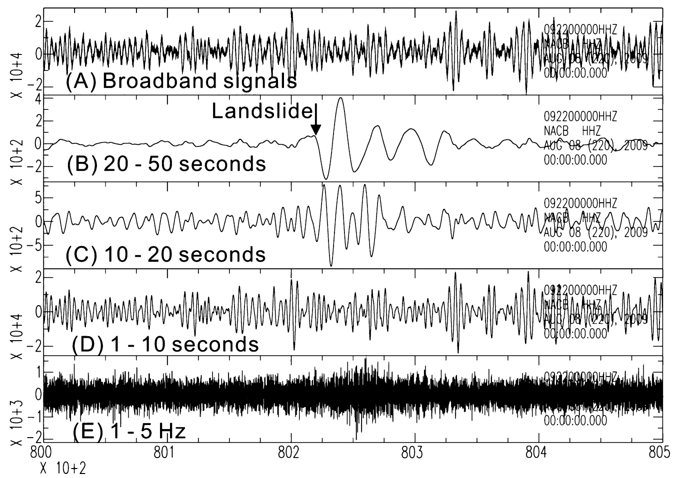

Fig. 1. An example showing the landslide earthquake that occurred at the Hsiaolin village and recorded at a distant station (NACB). The vertical seismograms from top to bottom are (a) original broadband, then band-passes of (b) 20–50 s, (c) 10–20 s, (d) 1–10 s and (e) 1–5 Hz. Landslide energy is clearly marked by an arrow at periods between 20 and 50 s.

In order to rapidly detect landslide seismic magnitude as well as location, we first analyzed all the large landslides that occurred during the period when Typhoon Morakot passed through Taiwan on August 7–10, 2009. We then defined landslide seismic magnitude based on an empirical formula. Similar to determining earthquake magnitude, the landslide seismic magnitude (**Lm**) is simply calculated according to both (1) the peak of seismic displacement recorded at broadband seismic stations and (2) the source distance between the seismic station and the landslide location. Thus, both the location and seismic magnitude of large landslides can be rapidly detected from broadband seismic networks for both academic and applied purposes in the future. Finally, some possible implications of the results of landslide statistics are discussed to improve our understanding of landslide seismology.

2. Landslide detection

Identification of very long period seismic signals generated by the rebound of the elastic crust after a landslide occurs near the surface provides reliable arrival times to locate the landslide source (Kanamori and Given, 1982; Kawakatsu, 1989; Ekstrom and Stark, 2013; Lin, 2015). After the 2009 Hsiaolin landslide in Taiwan (Lin et al., 2010), we showed that the broadband seismic network, whose original purpose is to routinely study earthquakes, could be useful for locating large landslides. An empirical band-pass filtering from 20 to 50 s (0.02–0.05 Hz) of the broadband seismic data can significantly enhance the seismic signals generated by large landslides. For instance, seismic signals generated by the Hsiaolin landslide and filtered by a variety of bands (0.2–1, 1–10, 10–20, 20–50 s) showed that landslide signals were largely dominated by very long period signals (20–50 s) (Fig. 1). During a 24 h period on August 8 (UTC), we successfully located 52 large landslides in Taiwan (Lin et al., 2010).

To detect more landslides that occurred during the entire period when Typhoon Morakot passed through Taiwan, in this study we have carefully examined all broadband seismic data and then identified all of the larger landslides during the time between August 7 and 10, 2009. Similar to the routine location of earthquakes, we have carefully read the arrivals of very long period seismic signals (20–50 s) at each station (Fig. 2). We have first compared every seismogram recorded at every station and then systematically picked the arrivals at the first maximum (peak) or minimum (trough) of the very long period seismic signals. It is very difficult to "miss-pick" the arrival time at each station because the adjacent maximum (or minimum) is more than 20 s early or late due to the very long period signals. Then we employed a least-square inversion algorithm (HYPO71, Lee and Jahr, 1972) to locate the source. Since the wavelengths of such long-period seismic signals are very long (∼150 km), a simple half-space model with a propagation velocity of 3.4 km/s was employed to calculate the travel-times from the landslide to the broadband seismic stations, based on a previous study (Lin et al., 2010) that showed that the very long period seismic signals are typically surface waves. For example, plots of very long period seismic signals versus station distances clearly show the propagation velocity is about 3.4 km/s in the Taiwan area (Fig. 2).

In fact, landslide events with very-long-period signals are easily distinguished from local earthquakes based on their frequency content as well as their wave propagation velocity (online supplement: Fig. S1). A local earthquake often generates strong high-frequency energy with small long-period signals, but a landslide only produces clear very-long-period energy without any recognizable high-frequency signal. During the period when Typhoon Morakot passed through Taiwan in 2009, no earthquakes were detected by the dense seismic stations in Taiwan as the landslides occurred. The apparent velocities recorded by a seismic network are also different between a local earthquake and landslide. The apparent velocity (∼ 3.4 km/s) of seismic waves generated by landslides (Fig. 2) is significantly less than that of local earthquakes. The very-long-period seismic signals (20–50 s) generated by the Hsiaolin landslide provide one of the best examples to distinguish landslides from earthquakes. In addition, both the location and time of the catastrophic landslide at the Hsiaolin village were clearly identified by eyewitnesses and in the scientific literature (Lin et al., 2010; Kuo et al., 2011; Chen et al., 2011; Tsou et al., 2011; Lin, 2015).

In total, we have detected 109 large landslides from August 7 to 10, 2009. Most of them were clustered in the mountainous area of southern Taiwan (Fig. 3), particularly in the Alishan area, where the accumulated rainfall was extremely high (>3000 mm). The general features of these clustered landslides are similar to previous studies (Lin et al., 2010; Chen et al., 2013). Although the estimated locations might not be exactly at the same sites as indicated from the field or via satellite images (Chen et al., 2013), the differences are relatively small and are acceptable for the purpose of rapid disaster response. For example, we have carefully examined the estimated locations of six larger landslides in this study with those marked by satellite imaging, and found that the errors ranged from 2.69 km to 7.92 km (online supplement: Fig. S2). The error for the Hsiaolin landslide was about 5.69 km.

3. Landslide seismic magnitude

In addition to locating 109 large landslides, we have defined the landslide seismic magnitude based on the relationship between the seismic displacements and source distances at different seismic stations. There are two major parameters for determining the landslide seismic magnitude. One is the maximum seismic amplitude recorded at the seismic stations; the other is the distance from the landslide to the stations. For example, plots of the maximum seismic amplitude recorded at different stations with their source distances on a log–log scale show extremely similar slopes of the regression lines from seven different landslides, as shown in Fig. 4. This result is similar to the seismic energy function of source-station distance obtained in Japan (Yamada et al., 2012).

This is analogous to estimating local seismic magnitude (M_L) at seismic stations (Richter, 1935), and therefore we have tried to formulate a landslide seismic magnitude (**Lm**) as below:

$$\mathbf{Lm} = \log(A) + \alpha \log(\Delta) + \beta \tag{1}$$

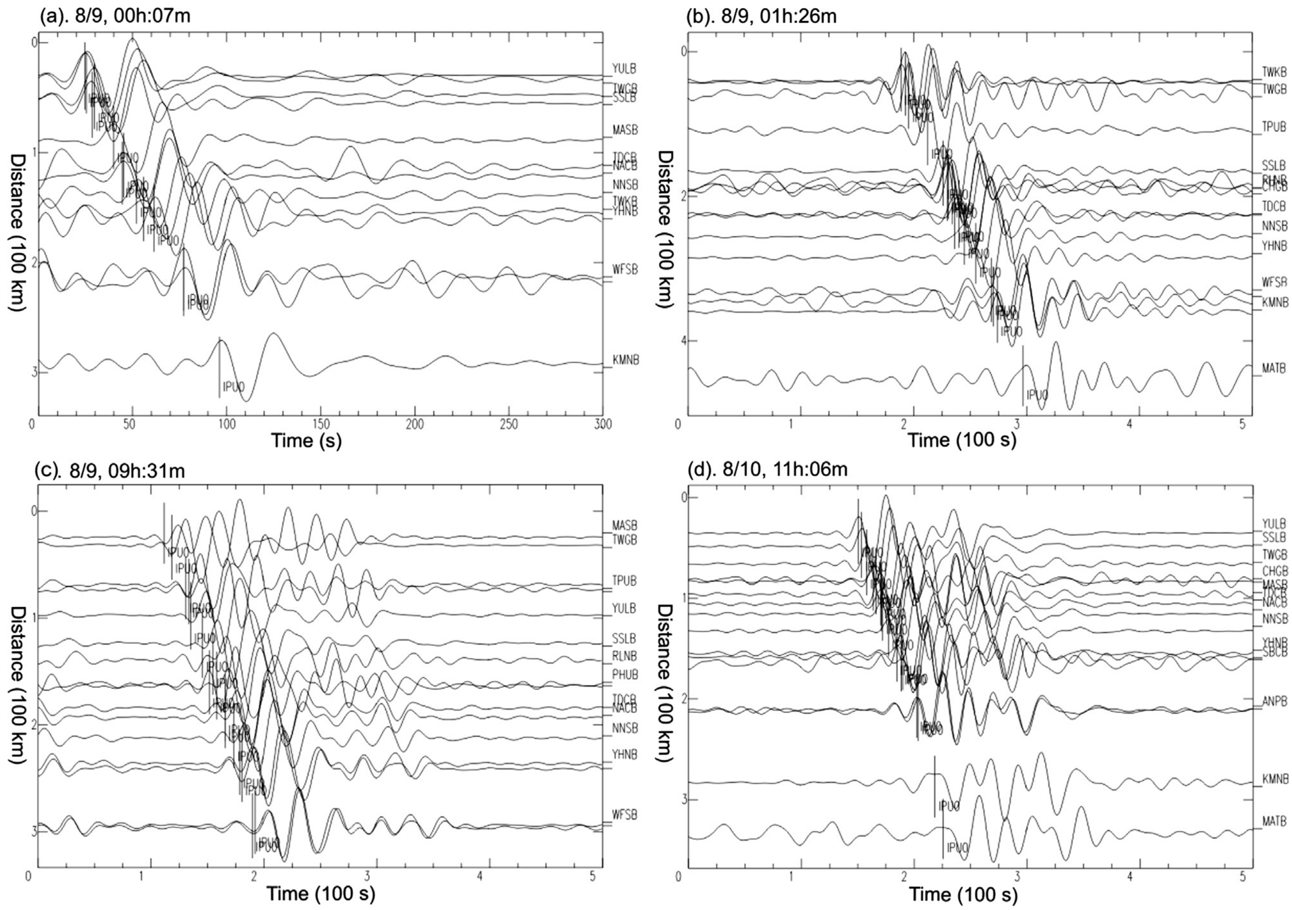

Fig. 2. Very long-period (20–50 s) seismograms generated by four larger landslides and recorded at broadband seismic stations in Taiwan when Typhoon Morakot passed Taiwan in August 2009 (UTC). The vertical bars labeled by IPU0 on each seismogram show the estimated arrival times at each station. Among them, the largest landslide (**Lm** = 4.3) at 9:31AM, August 9 is shown in Fig. 2c.

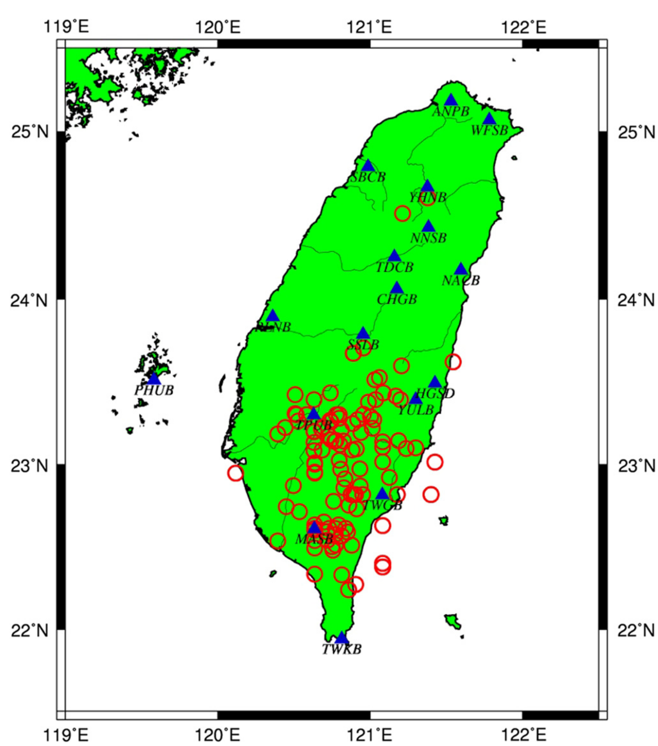

Fig. 3. Broadband seismic stations (triangles) and calculated locations (circles) of 109 large landslides that occurred between August 7 and 10 when Typhoon Morakot struck Taiwan in 2009.

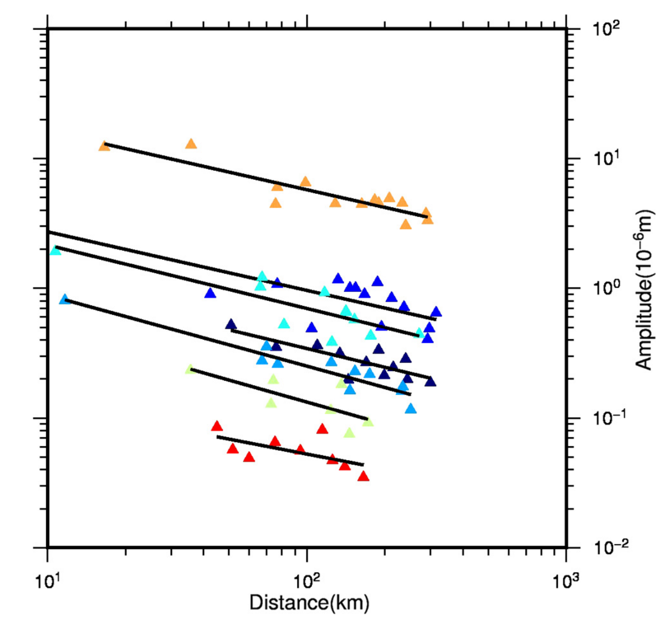

Fig. 4. Plots of maximum amplitudes recorded by seismic stations at different distances in the log–log scale from seven landslides, marked in different colors. The lines show the least-square regression for each landslide.

where A is the maximum displacement (μm) of the extremely long period (20–50 s) signal on the vertical component measured at a seismic station, Δ is the distance (km) between the landslide and the station, and both α and β are constants. For each landslide we

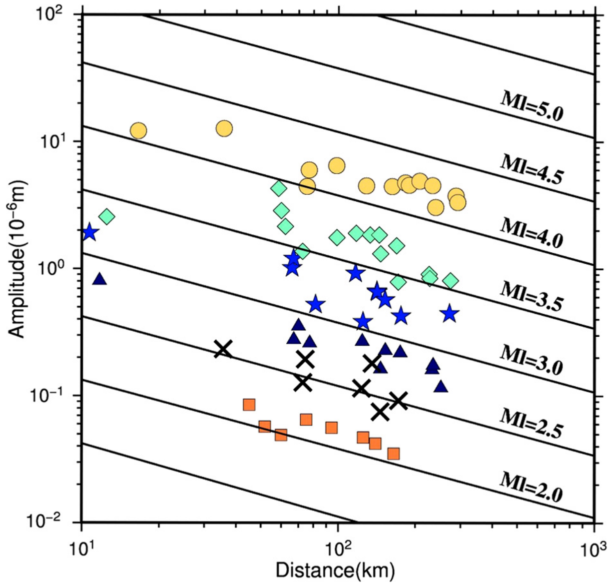

Fig. 5. Empirical relationships between source distances and seismic displacements generated by different magnitude landslides (**Lm**) roughly ranging from 2.2 to 4.3. Different symbols show seismic amplitudes of six landslides recorded at distances between 10 and 300 km.

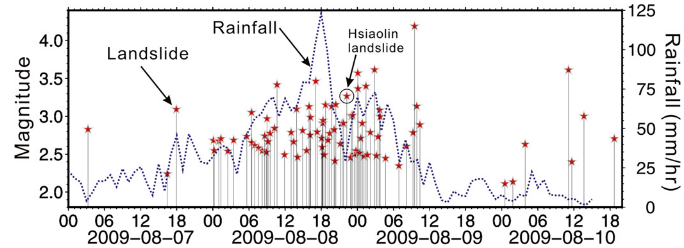

Fig. 6. Temporary variations of landslide magnitudes (stars) and rainfall (dashed line) recorded at Alishan in southern Taiwan during the period between August 7 and 10, 2009 (UTC). The Hsiaolin landslide with a magnitude (**Lm**) of 3.4 is marked in green. (For interpretation of the references to color in this figure legend, the reader is referred to the web version of this article.)

have plotted all maximum displacements recorded at every station with its distance on the log–log scale (Fig. 4). Then a constant α can be determined from the slope of the regression line of the maximum displacements measured at different distances. Although the estimated α values are distributed from 0.85 to 0.35 among 88 landslides, statistical analysis shows the average of α is 0.55 with a standard deviation of 0.12.

In order to obtain the constant β in equation (1), we selected the well-studied landslide that occurred at Hsiaolin village to constrain the landslide seismic magnitude (**Lm**) from the seismic moment estimation. We simply assumed that the landslide seismic moment (M_o) is a result of the force applied at the landslide multiplied by the landslide slip along its path. Based on the source inversion result (Lin et al., 2010), the Hsiaolin landslide was pushed by a single force of $\sim 5.0 \times 10^{10}$ (N). If we consider that the total slide distance was about 3000 m (Tsou et al., 2011), then the seismic moment (M_o) was about 1.5×10^{14} N m or 1.5×10^{21} dyn cm. Although the source mechanism for earthquakes and landslides is different, we further defined the moment seismic magnitude (M_w) as about 3.4 based on the equation $M_w = 2/3 \times \log(M_o) - 10.7$ (Hanks and Kanamori, 1979). Then we defined the moment seismic magnitude (M_w) as equivalent to the landslide seismic magnitude (**Lm**) in equation (1), resulting in a constant β of about 2.44.

Finally, we obtained an empirical formula for estimating landslide seismic magnitude in general: $\mathbf{Lm} = \log(A) + 0.55\log(\Delta) + 2.44$; where A is the vertical maximum displacement (μm) of the long-period seismic signals (20–50 s) measured at one seismic station, and Δ is the distance (km) between the landslide and the station. Fig. 5 shows examples of six landslides with seismic magnitudes (**Lm**) roughly ranging from 2.2 to 4.3 observed at distances from 10 km to 300 km. Thus, the empirical formula (**Lm**) can be directly used for estimating large landslides observed by broadband seismic networks in Taiwan. It might also be modified for application in other areas based on their geological features.

4. Landslide statistics

Based on the empirical formula, the seismic magnitudes (**Lm**) of 109 landslides that occurred from August 7 to 10, 2009 (UTC time) have been plotted with time (Fig. 6). Most of them were clustered around August 8 and early August 9, when the rainfall was extremely heavy in most of the southern Taiwan area. It is also worth noting that eight of these landslides were larger than the Hsiaolin landslide (**Lm** = 3.4), even though they caused no significant damage. Both the magnitude and number of the larger landslides roughly increased with time from August 8 to early August 9. The largest one (**Lm** = 4.2) occurred at 9AM on August 9. After the largest landslide, there were almost no large landslides until August 10, when a few large landslides occurred again. This phenomenon is roughly consistent with a significant reduction of the accumulated rainfall during this period.

It is interesting to note that, similar to an early earthquake study (Gutenberg and Richter, 1942), there is an empirical relation between the frequency and magnitude of landslides:

$$\log N(\mathbf{Lm}) = a - b m_L \tag{2}$$

where a and b are constants, **Lm** is the landslide seismic magnitude, and N(**Lm**) is the number of landslides with magnitude greater than **Lm** in a specific time window. Although the smallest landslide magnitude was 2.1, we have obtained a seismic b-value of 1.23 and a-value of 5.19 based on identified landslides with magnitudes between 2.5 and 4.1 (Fig. 7). The formal uncertainty of the b-value ranges from 1.11 to 1.36 based on the 90% of Student's t-distribution for the regression. However, the steep slope is largely determined by the two data points at magnitudes 3.8 and 4.0, which are defined by only two events; thus more data are needed before this result can be considered robust. The b-value of 1.23 is significantly higher than a normal b-value ($\sim$1.0) often obtained from earthquakes in Taiwan (Wang, 1988), but extremely similar to the seismic b-values of seismic swarms observed at volcanic or geothermal areas (Konstantinou et al., 2007; Kim et al., 2005). Since this is the first time obtaining a landslide b-value from limited data, it is hard to justify the landslide b-value of 1.23 as either a typical or unusual characteristic at this moment. More observations have to be conducted to discuss seismic b-values of landslides in the near future.

5. Discussion

It is interesting to note that the constants $\alpha = 0.55$ and $\beta = 2.44$ obtained in equation (1) for estimating landslide seismic magnitude (**Lm**) are quite different from those used for calculating local earthquake magnitudes (M_L) (Richter, 1935) below:

$$\text{Earthquake magnitude: } M_L = \log(A) + 2.76\log(\Delta) - 2.48 \tag{3}$$

$$\text{Landslide magnitude: } \mathbf{Lm} = \log(A) + 0.55\log(\Delta) + 2.44 \tag{4}$$

Both values ($\alpha = 2.76$ and $\beta = -2.48$) for determining local earthquake magnitude (M_L) in Equation (3) are significantly different

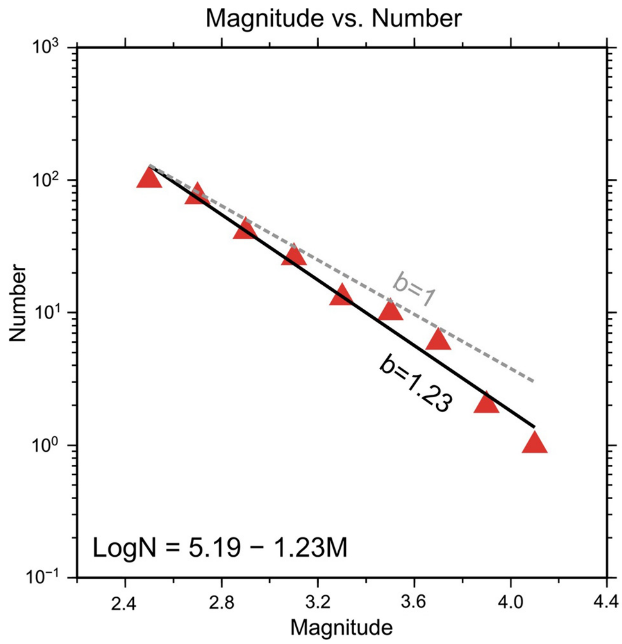

Fig. 7. Plot of observations (triangles) and the regression slope ($b = 1.23$) of landslide magnitudes vs. log (numbers) during the period between August 7 and 10, 2009. A reference slope of $b = 1.0$ is also shown by a dashed line.

from those for estimating landslide seismic magnitude (**Lm**) in Equation (4). An obvious possible reason is that the decay of extreme long-period seismic waves (20–50 s) generated by landslides is significantly less than that of short-period seismic waves (1–5 Hz) generated by local earthquakes. It is well known that the decay of seismic waves is strongly dependent on their periods. Seismic energy of longer period signals decays with distance slower than that of shorter period signals. In addition, seismic energy generated by landslides is largely trapped near the surface since the source is almost on the surface. This is completely unlike earthquakes, whose energy is released more efficiently into the deep earth because the source is a certain depth underground. The small decay of seismic energy generated by landslides provides a significant advantage in detecting landslides using broadband seismic stations in that the landslides can be more efficiently detected at remote distances. For the same energy released by an earthquake and landslide, the latter might be more easily detected by distant seismic stations than the former. For example, seismic waves generated by the Hsiaolin landslide (**Lm** = 3.4) clearly propagated more than 2000 km and were well recorded at broadband seismic stations in Japan (Lin et al., 2010).

The mechanism of landslide generation observed in this study is more similar to seismic swarms in volcanic or geothermal areas than general earthquakes in the fault zones. At first, a high seismic b-value of 1.23 was obtained from calculations based on more than 100 large landslides that occurred in the southern Taiwan area during 2009 when Typhoon Morakot passed through Taiwan, which is significantly higher than a typical b-value of around 1.0 obtained from earthquakes in fault zones or general areas. Instead, this high b-value is more similar to that of earthquakes observed at volcanic or geothermal areas. In other words, the high b-value of 1.23 obtained from landslides implies that most landslides occurred with a similar magnitude and within four days. Secondly, the temporal behavior of large landslides (Fig. 7) also suggests that landslides are characteristically more like seismic swarms than typical earthquake sequences, which are often characterized by many smaller aftershocks triggered by the main-shock. Here we found that smaller landslides did not always follow larger landslides. On the other hand, some landslides increased in magnitude with time during one particular period around August 8. All of these features suggest that most landslides of similar sizes and extremely similar conditions, including geological background (rocks, fractures, beddings and faults) as well as weather conditions (rainfalls and air pressure), occur when a triggering level is reached.

Based on the analyses above, rapid detection of landslide source parameters, including location, time and seismic magnitude, can be achieved using real-time data recorded at a broadband seismic network. First, the occurrence time and location of large landslides can be calculated from the arrival times of the long-period seismic signals recorded by the network. Second, the landslide earthquake magnitude obtained from Equation (4) provides a rapid estimation of landslide seismic magnitude. This is very useful not only for academic study, but also for disaster prevention. For academic purposes, it is useful for identifying landslide source parameters for further investigation. For disaster prevention, the detection of large landslides from seismic networks provides first-hand information to (1) evaluate possible disasters, (2) make a rescue plan if necessary and (3) schedule a further detailed survey. Although there are still some uncertainties regarding location and seismic magnitude, it provides the most rapid information needed to carry out high-resolution imaging by aircrafts or satellites over a limited area. Otherwise, a grid-search image without a clear target or area will become an extremely time-consuming effort that may obtain only low-resolution results.

We recommend that an automatic detection system for landslides using broadband seismic networks be established in many areas where landslides occur frequently, particularly areas in which seismic networks are available for detecting earthquakes such as Taiwan, Japan, Italy, and New Zealand. For the areas where seismic networks are not ready, the installation of a few seismic stations might be important for multiple reasons, such as detecting landslides rapidly as well as seismological studies.

6. Conclusion

Careful examination of long-period seismic data generated by large landslides and recorded at a broadband seismic network on August 7–10, 2009 when Typhoon Morakot passed through Taiwan showed that the source parameters (time, location and seismic magnitude) of large landslides can be rapidly calculated by an empirical equation, $\mathbf{Lm} = \log(A) + 0.55\log(\Delta) + 2.44$, where A is the maximum displacement (μm) recorded at each seismic station and Δ is its distance (km) from the landslide. Furthermore, the seismic b-value of 1.23 obtained from more than 100 landslides indicated that the mechanism of landslide generation observed in this study is more like seismic swarms in volcanic or geothermal areas than general earthquakes in fault zones. This feature suggests that most landslides of similar sizes and extremely similar conditions (including geological background and weather conditions) might occur when a triggering level is reached. Finally, we suggest that a real-time algorithm should be set up to routinely monitor landslides in places where landslides are a frequent threat, such as in Taiwan, Japan, Italy, and New Zealand.

Acknowledgement

The authors would like to thank the Central Weather Bureau and Institute of Earth Sciences, Academia Sinica in Taiwan as well as the National Research Institute for Earth Science and Disaster Prevention in Japan for providing the broadband seismic data in the Taiwan area. The financial support from the Ministry of Science and Technology, R.O.C. and the Sustainability Center of Academia Sinica in R.O.C. is also appreciated. The invitation for the first author to visit the Institute of Seismology and Volcanology, Hokkaido University was really helpful for completing this manuscript. We are very appreciated at the valuable comments and suggestions by both anonymous reviewer and the editor (P. Shearer) for improving the paper.

Appendix A. Supplementary material

Supplementary material related to this article can be found online at http://dx.doi.org/10.1016/j.epsl.2015.07.068.

References

Chen, C.C., Dong, J.J., Kuo, C.Y., Hwang, R.D., Li, M.H., Lee, C.T., 2011. Reconstruction of the kinematics of landslide and debris flow through numerical modelling supported by multidisciplinary data: the 2009 Siaolin, Taiwan landslide. In: Bhuiyan, F. (Ed.), Sediment Transport – Flow and Morphological Processes. ISBN 978-953-307-374-3.

Chen, C.H., Chao, W.A., Wu, Y.M., Zhao, L., Chen, Y.G., Ho, W.Y., Lin, T.L., Kuo, K.H., Chang, J.M., 2013. A seismological study of landquakes using a real-time broadband seismic network. Geophys. J. Int. 194 (2), 885–898.

Ekström, G., Stark, C.P., 2013. Simple scaling of catastrophic landslide dynamics. Science 339 (6126), 1416–1419. http://dx.doi.org/10.1126/science.1232887.

Gutenberg, B., Richter, C.R., 1942. Earthquake magnitude, intensity, energy and acceleration. Bull. Seismol. Soc. Am. 32, 163–191.

Hanks, T., Kanamori, H., 1979. A moment magnitude scale. J. Geophys. Res. 84, 2348–2349.

Kanamori, H., Given, J.W., 1982. Analysis of long-period seismic waves excited by the May 18, 1980, eruption of Mount St. Helens – a terrestrial monopole? J. Geophys. Res. 87, 5422.

Kawakatsu, H., 1989. Centroid single force inversion of seismic waves generated by landslides. J. Geophys. Res. 94, 12363–12374.

Kim, K.H., Chang, C.H., Ma, K.F., Chiu, J.M., Chen, K.C., 2005. Modern seismic observations in the Tatun volcano region of northern Taiwan: seismic/volcanic hazard adjacent to the Taipei metropolitan area. Terr. Atmos. Ocean. Sci. 16 (3), 579–594.

Konstantinou, K.I., Lin, C.H., Liang, W.T., 2007. Seismicity characteristics of a potentially active Quaternary volcano: the Tatun volcano group, northern Taiwan. J. Volcanol. Geotherm. Res. 160, 300–318.

Kuo, C.Y., Tsai, Y.C., Chen, C.C., Chang, K.J., Siau, A.Y., Dong, J.J., Han, R.H., Shimamoto, T., Lee, C.T., 2011. The landslide stage of the Hsiaolin catastrophe: simulation and validation. J. Geophys. Res. 116, F04007. http://dx.doi.org/10.1029/2010JF001921.

Lee, W.H.K., Jahr, J.C., 1972. A computer program for hypocenter, magnitude and first motion pattern of local earthquakes. USGS open file report.

Lin, C.H., 2015. Insight into landslide kinematics from broadband seismic network. Earth Planets Space 67 (8). http://dx.doi.org/10.1186/s40623-014-0177-8.

Lin, C.H., Kumagai, H., Ando, M., Shin, T.C., 2010. Detection of landslides and submarine slumps using broadband seismic networks. Geophys. Res. Lett. 37, L22309. http://dx.doi.org/10.1029/2010GL044685.

Richter, C.F., 1935. An instrumental magnitude scale. Bull. Seismol. Soc. Am. 25, 1–32.

Tsou, C.Y., Feng, Z.Y., Chigira, M., 2011. Catastrophic landslide induced by Typhoon Morakot, Shiaolin, Taiwan. Geomorphology 127, 166–178.

Wang, J.H., 1988. *b*-values of shallow earthquakes in Taiwan. Bull. Seismol. Soc. Am. 78, 1243–1254.

Yamada, M., Matsushi, Y., Chigira, M., Mori, J., 2012. Seismic recordings of landslides caused by Typhoon Talas (2011), Japan. Geophys. Res. Lett. 39, L13301. http://dx.doi.org/10.1029/2012GL052174.